



研究論文

Simultaneous Measurement of an Electron Density Profile and a Density Fluctuation Using Ultrashort-Pulse Reflectometry

ITAKURA Akiyosi, KATOH Masayuki, KUBOTA Shigeyuki¹⁾, MASE Atsushi²⁾,
ONUMA Tsuyoshi³⁾, HOJO Hitoshi and YATSU Kiyoshi
Plasma Research Center, University of Tsukuba, Tsukuba 305-8577, Japan

(Received 28 February 2000 / Accepted 28 September 2000)

Abstract

An ultrashort-pulse reflectometry using an ordinary mode (O-mode) wave is applied to the GAMMA 10 device. A microwave probing signal is generated by an impulse generator with a pulse width of 65 ps. The signal is transmitted by a pyramidal horn and has a broad frequency spectrum. Different frequency components are reflected at corresponding cutoff layers in the plasma. The reflected wave is received by an adjacent pyramidal horn and is divided into five frequency channels: 7, 8, 9, 10 and 11 GHz. The time-of-flight for each channel is measured using a time-to-amplitude converter. An electron density profile is reconstructed with one-shot data. A radial distribution of density fluctuation is observed simultaneously.

Keywords:

microwave diagnostics, reflectometry, ultrashort-pulse, time-of-flight, electron density profile, density fluctuation

1. Introduction

For a fusion-oriented plasma, a microwave interferometer has been a standard tool for measuring the electron density. The frequency of the probe beam is selected to be higher than the cutoff frequency to avoid the effect of reflection. Reflectometry, on the other hand, utilizes the cutoff effect [1,2]. Since one probing frequency measures one cutoff layer, it requires a microwave source having a wide frequency range. With recent developments in semiconductor oscillators, microwave reflectometry has become a potential tool for

realizing local measurements of density and fluctuation. A wide range of frequencies is realized by several methods. One promising method is a fast frequency sweep of an oscillator, or in another word, frequency modulation [3,4]. This method has the advantage of being able to neglect density fluctuations using a high-speed sweep. The beat frequency of the receiving system can be chosen adequately by adjusting the path difference between the probing signal and the reference signal, and the sweep rate of the oscillator. But the adjustment is rather complicated because the tuning

author's e-mail: itakura@prc.tsukuba.ac.jp

1) Present address: Department of Physics, University of California, Los Angeles, CA 90095, USA

2) Present address: Advanced Science and Technology Center for Cooperative Research, Kyushu University, Kasuga 816-8580, Japan

3) Present address: Tsukuba Research Laboratory, Hitachi Maxell, Ltd., Yawara 300-2496, Japan

sensitivity of the oscillator is nonlinear.

On the other hand, an ultrashort-pulse has a broad frequency spectrum. Therefore, the system needs only one generator [5,6]. The receiving system must be able to detect several frequency channels. In this paper, a five-channel system is described. The time-of-flight for each channel is measured. The electron density profile is derived from the time-of-flight measurements from a single shot. Since the fluctuation in the time-of-flight means a deviation of the cutoff layer, the frequency spectrum of density fluctuation is observed simultaneously. The experimental apparatus and method are described in Sec.2. The experimental results are described and discussed in Sec.3, and are summarized in Sec.4.

2. Experimental Apparatus and Method

Figure 1 shows a schematic diagram of the ultrashort-pulse reflectometer installed in the GAMMA 10 device [7]. A detailed description of the system is given by Kubota et al. [8] for a four-channel system. Radial profiles of the characteristic frequencies in the GAMMA 10 are also shown in the Ref. 8. The microwave source

is an impulse generator (Picosecond Pulse Labs 3500D) with a pulse width of 65 ps FWHM (Full Width Half Maximum). The impulse is fed into an amplifier through a waveguide for waveform shaping. It is launched from a pyramidal horn in the ordinary mode (O-mode). The signal reflected by the plasma cutoff layer is received by a horn of the same type and is amplified by a preamplifier. It is then divided into 5 channels and frequency-selected by band-pass filters with central frequencies of 7, 8, 9, 10 and 11 GHz, each having a bandwidth of 3% of the central frequency. They are detected by Schottky barrier diodes, amplified and fed into a time-of-flight measurement system. The time-of-flight is measured by a time-to-amplitude converter (ORTEC 566), whose time resolution is within 0.01% of full scale 50 ns. The converter is started by the impulse generator, which is synchronized with the clock of the 12 bit analog to digital converter (Jorway Aurora 14), and stopped by the discriminator output signal of each channel. The output amplitude of the converter is proportional to the time-of-flight and is converted again to a digital signal, and transferred to a data acquisition system. These data are processed after a shot using

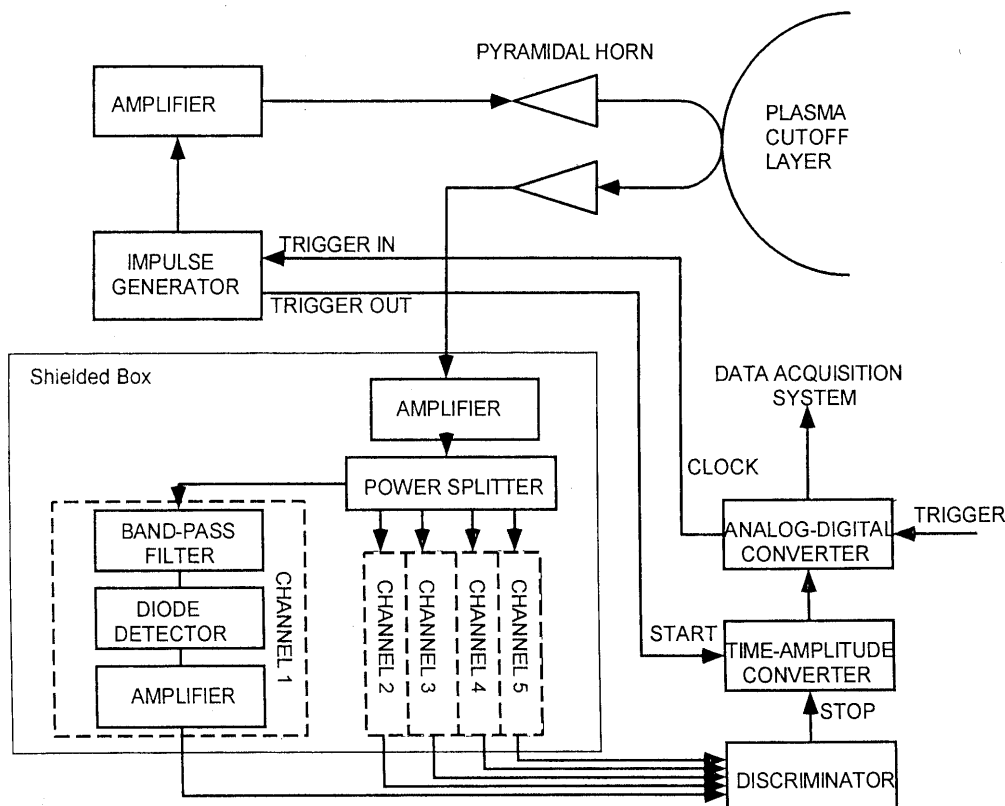


Fig. 1 Schematic diagram of the ultrashort-pulse reflectometer.

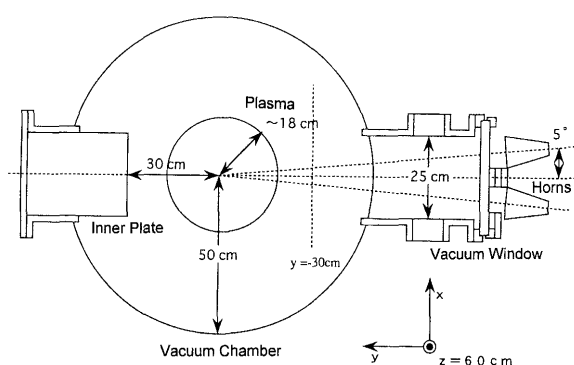


Fig. 2 Cross sectional view of the central cell and the reflectometer horns.

MATLAB software. Total time resolution of the system is smaller than 0.01 ns, but measurement error is about 10 time larger than that.

This system is located at a distance of 0.6 m from the midplane of the central cell. The cross section of this point is shown in Fig. 2. The launching and receiving horn system is attached to a horizontal window.

3. Experimental Results and Discussions

3.1 Density profile

Figure 3(a) shows a time evolution of line integrated electron density obtained by an interferometer. The plasma discharge is initiated by plasma guns located at both ends of the device at 50.5 ms. The plasma is produced and sustained by ion cyclotron range of frequency (RF) applied in the central cell. Electron cyclotron resonance heating (ECRH) for formation of plug potential is applied from 125 ms to 225 ms by two sets of gyrotrons.

The round trip time-of-flight $\tau(f)$ for frequency f between vacuum window y_w and reflection point y_r is deduced [3] as

$$\tau(f) = \frac{2}{c} \int_{y_w}^{y_r} \left[1 - \left(\frac{f_{pe}}{f} \right)^2 \right]^{-\frac{1}{2}} dy, \quad (1)$$

$$f_{pe} = \frac{1}{2\pi} \left(\frac{e^2 n_e}{\epsilon_0 m_e} \right)^{\frac{1}{2}}, \quad (2)$$

where f_{pe} is the electron plasma frequency for the electron density n_e , ϵ_0 is the permittivity of vacuum, c is the velocity of light, e is the electron charge and m_e is the electron mass. The time-of-flight measured for each frequency component is shown in Fig. 3(b). When the

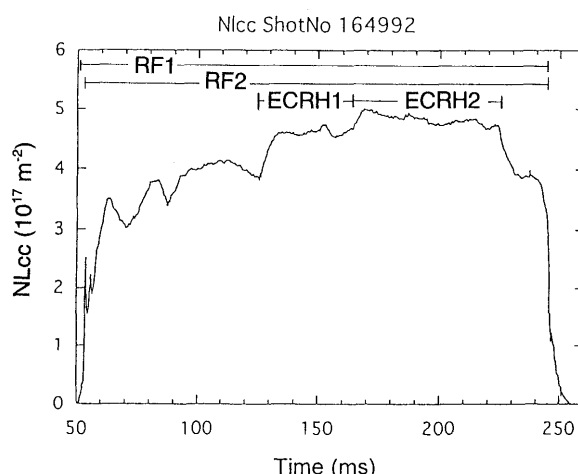


Fig. 3(a) Line integrated electron density, NLcc (10^{17}m^{-2}) as a function of time.

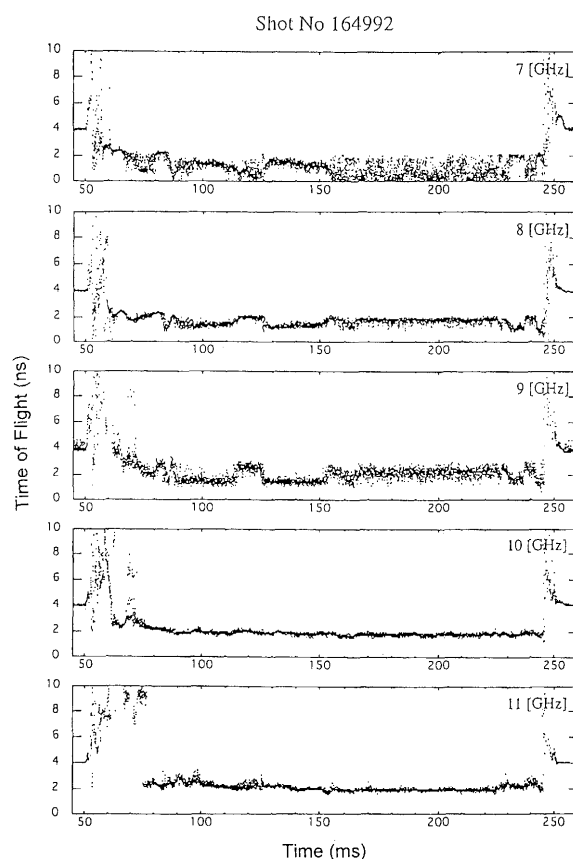


Fig. 3(b) Time-of-flight of each receiving frequency as a function of time.

plasma does not exist, probe beam is reflected on the inner plate in the vacuum chamber. The base line of the time-of-flight is set at $y = -0.3 \text{ m}$ in Fig. 2 for convenience of calculation. Without plasma during 47 ms and

49 ms, measured values are averaged and normalized as 4 ns. A scanning interferometer is installed in the central cell of the GAMMA 10. Kubota *et al.* [8] show that the measured time-of-flight roughly coincides with the calculated value from the density distribution, which is derived from the line integrated density profile obtained by the scanning interferometer. Measured data are averaged for 1 ms to avoid the effects of noise and fluctuations, though the analog to digital converter takes data every 8 μs . The density distribution at a certain time is derived as follows. The time-of-flight profile is approximated as a polynomial function of frequency at a given time. Figure 4 shows the deduced relation at $t = 100$ ms. Then the density profile is derived from this curve with the assumption that the density at radial location $y = -0.18$ m is 0, because the radius of central cell limiter is 0.18 m. This is plotted in Fig. 5(a). Conversion of the time-of-flight to the density profile has some ambiguity, because the density distribution itself is based on an approximation. A calibration is performed using the scanning interferometer, which is located at the equal distance from the midplane in the opposite direction of the central cell. In Fig. 5(b), the solid line is the profile deduced by the scanning interferometer from 10 different shots showing nearly equal line integral densities. Here, radial positions shown in crosses are deduced from the time-of-flights and are scaled down by 0.82, so as to minimize the difference. In this system the maximum receiving frequency is 11 GHz, so that densities higher than $1.5 \times 10^{18} \text{ m}^{-3}$ cannot be obtained. The dashed line is the extrapolated radial profile deduced from the time-of-flight. This profile shows the peak density 2.0×10^{18}

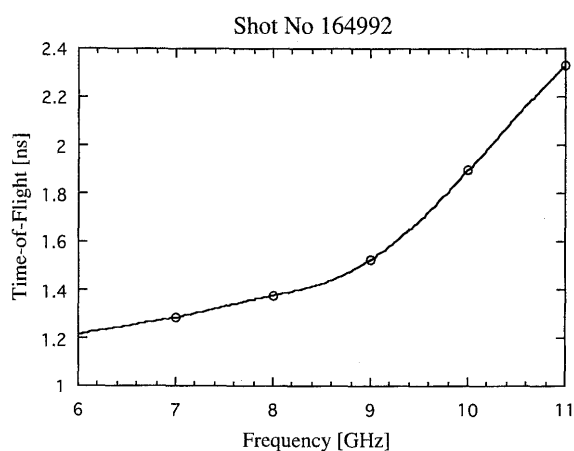


Fig. 4 Time-of-flight versus frequency at time 100 ms.

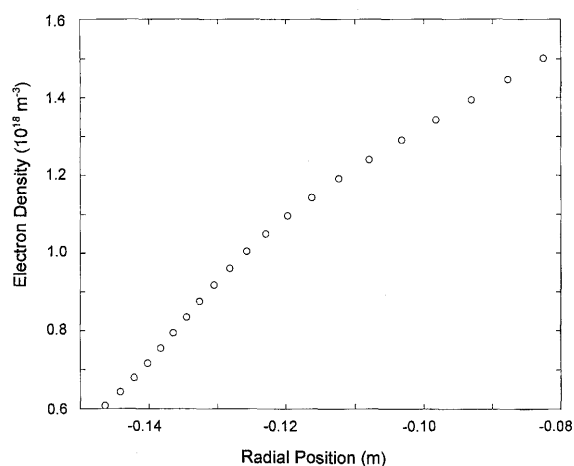


Fig. 5(a) The electron density profile derived from the time-of-flight shown in Fig. 3.

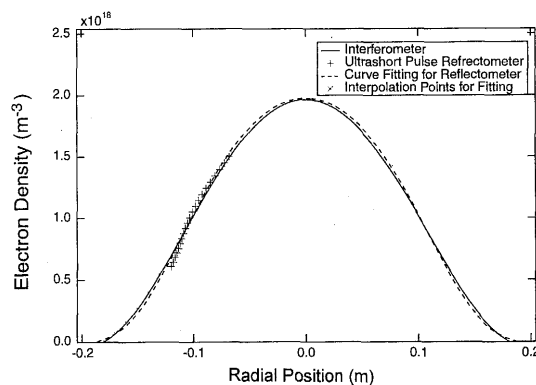


Fig. 5(b) The electron density profiles at 100 ms. Plus signs are derived from the time-of-flight. Dashed line is the extrapolation of plus signs. Solid line is derived from the scanning interferometer in other 10 shots.

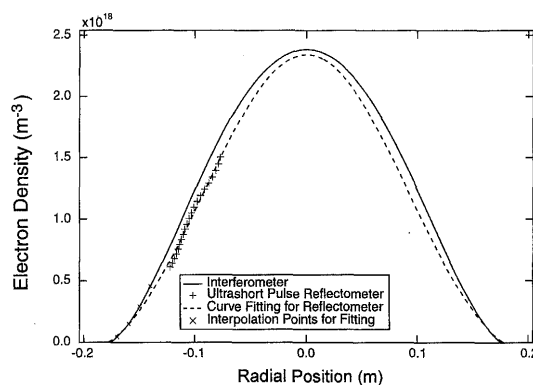


Fig. 6 The electron density profiles at 140 ms. Notes are the same as in Fig. 4(b).

m^{-3} . Using this calibration coefficient, density profile at the time 140 ms is shown in Fig. 6, and it shows fairly good agreement with the result of the interferometer. The difference becomes smaller after further optimization of the density profile from the time-of-flight. A detailed study of the time dependence of the density profile is shown elsewhere.

3.2 Fluctuation measurements

The scatter of the data points in Fig. 3(b) shows that there is a fluctuation in the time-of-flight, i.e., a fluctuation in the location of the cutoff layer. The clock frequency of the analog-to-digital converter is 250 kHz, however the data are effectively sampled at 125 kHz, since the time-to-amplitude converter requires a clock cycle to acquire the data and a clock cycle to output the data. The signal is frequency analysed using the Lomb periodogram [9]. The time-to-amplitude converter sometimes misses a trigger and does not generate a signal. The Lomb periodogram has an advantage over the usual FFT (Fast Fourier Transform) method with the spectral analysis of unevenly sampled data. Figure 7 shows the frequency spectra at time $t = 100$ ms. "Channel-Freq" in the figure corresponds to the cutoff density, i.e., radial location. Fluctuations around 4 kHz have the maximum amplitude and are located on 8 GHz channel. The cutoff density at 8 GHz is $0.8 \times 10^{18} \text{ m}^{-3}$. Spectra are truncated at 45 kHz, because there is some system noise at 50 kHz. The fluctuation level is maximum on the 10 GHz signal, which corresponds to a cutoff density of $1.2 \times 10^{18} \text{ m}^{-3}$. Low frequency waves have been investigated using the Fraunhofer diffraction method, when there exists an $\mathbf{E} \times \mathbf{B}$ rotation of plasma

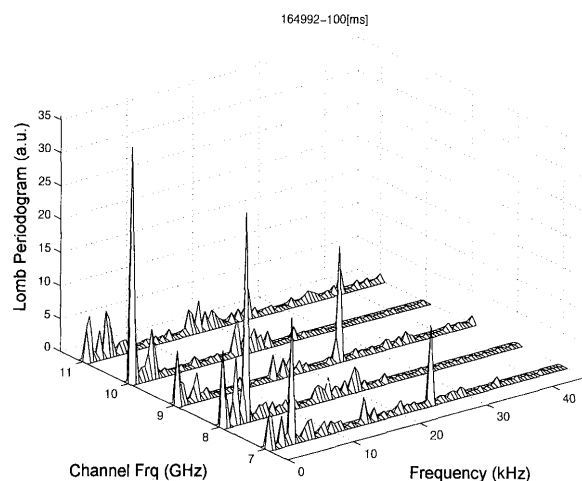


Fig. 7 Frequency spectra of density fluctuations at time 100 ms.

[4]. Fluctuations obtained here seem to be of the same kind. A detailed analysis will be appeared in a separate paper.

4. Summary

An ultrashort-pulse reflectometer is installed in the GAMMA 10 device. The electron density profile can be obtained from a single shot. As an O-mode system with a maximum receiving frequency of 11 GHz, density profiles can be measured for about half the radius of the plasma. By extending the frequency range of the receiving system and combining with an X-mode horn system, a wider range of densities can be probed. In addition, the density fluctuation spectrum can be measured simultaneously with the density profile.

Acknowledgements

The authors are greatly indebted to Mr. Y. Kogi and the members of Plasma Research Center, University of Tsukuba, for their help in the experiment. They also acknowledge Dr. C.W. Domier, University of California at Davis, USA, for his cooperation.

References

- [1] I.H. Hutchinson, *Principles of Plasma Diagnostics* (Cambridge University Press, 1990) p.125.
- [2] A. Mase, T. Tokuzawa, L.G. Bruskin, Y. Kogi *et al.*, *J. Plasma Fusion Res.* **74**, 1189 (1998).
- [3] J.L. Doane, E. Mazzucato and G.L. Schmidt, *Rev. Sci. Instrum.* **52**, 12 (1981).
- [4] T. Tokuzawa, A. Mase, N. Oyama, A. Itakura and T. Tamano, *Rev. Sci. Instrum.* **68**, Pt.II, 443 (1997).
- [5] C.W. Domier, N.C. Luhmann, Jr., A.E. Chou, W-M. Zhang and A.J. Romanowsky, *Rev. Sci. Instrum.* **66**, 399 (1995).
- [6] S. Kubota, T. Onuma, M. Katoh, A. Mase *et al.*, *Jpn. J. Appl. Phys.* **38**, Pt.2, L202 (1999).
- [7] K. Yatsu, L.G. Bruskin, T. Cho, M. Hamada *et al.*, *J. Plasma Fusion Res.* **74**, 844 (1998).
- [8] S. Kubota, T. Onuma, M. Kato, A. Mase *et al.*, *Rev. Sci. Instrum.* **70**, Pt.II, 1042 (1999).
- [9] W.H. Press, S.A. Teukolsky, W.T. Vetterling and B.P. Flannery, *Numerical Recipes in C: The Art of Scientific Computing*, 2nd ed. (Cambridge University Press, 1995) p.575.